

Preliminary three-dimensional numerical analyses of South Peak area, Turtle Mountain, Alberta



Marc-André Brideau¹; Andrea Pedrazzini²; Doug Stead¹; Michel Jaboyedoff²; Corey Froese³

1. Department of Earth Science, Simon Fraser University, Burnaby, British Columbia

2. Institut de Geomatique et d'Analyse du Risque, Université de Lausanne, Lausanne, Suisse

3. Alberta Geological Survey/Energy Resources Conservation Board, Edmonton, Alberta

ABSTRACT

The South Peak area on Turtle Mountain is located adjacent to the 1903 Frank Slide. The objectives of this paper are to present three-dimensional numerical models and compare them with previous conceptual models based on discontinuity surfaces identified using airborne LiDAR. The slope analysis methodology applied included evaluating probable simple discontinuity-controlled failure modes using kinematic analysis and assessing the potential for wedge failure through a limit equilibrium combination analysis. Block theory was used to evaluate the finiteness and removability of blocks in the rock mass. The complex interaction between discontinuity sets within South Peak and the topography was finally investigated through preliminary three-dimensional distinct element models.

RÉSUMÉ

La partie South Peak de Turtle Mountain est située immédiatement au sud du glissement Frank survenu en 1903. L'objectif de cet article est de présenter des modèles numériques tridimensionnels et de les comparer avec un modèle conceptuel basé sur des surfaces de discontinuités identifiées à partir de LiDAR aérien. Les méthodes d'analyses de pente utilisées incluent l'analyse cinématique pour évaluer les mécanismes de rupture simple et la méthode d'équilibre limite en combinaison ont été utilisées pour évaluer le potentiel de rupture en dièdre. La théorie des blocs clefs a été utilisée pour évaluer la finité et la facilité de déplacement des blocs dans la masse rocheuse. Les interactions complexes entre les discontinuités présentes et la topographie ont été étudiées par la modélisation tridimensionnelle préliminaire d'éléments distincts.

1 INTRODUCTION

The South Peak area on Turtle Mountain is located adjacent to the 1903 Frank Slide. A 5-Mm³ section of South Peak is considered unstable and a real-time monitoring system was installed in 2003 (Moreno and Froese, 2006). As part of an ongoing research program on Turtle Mountain led by the Alberta Geological Survey, structural geology measurements, rock mass descriptions and rock samples were collected in the South Peak area in 2008.

Turtle Mountain is located in southern Alberta (Figure 1), and is composed of folded Paleozoic and Mesozoic sedimentary rocks (Cruden and Krahn, 1973; Langenberg et al., 2007). The dominant structure in the upper part of the mountain is the Turtle Mountain anticline (Figure 2). The role of thrusts and mining in the lower section of the Turtle Mountain on the 1903 slope failure has been investigated by Benko and Stead (1998) and Cruden and Martin (2007).

The conceptual deformation model for the South Peak area presented in Figure 3 was constructed based on the discontinuity surfaces identified in the airborne LiDAR data using the COLTOP 3D software, and field observations (Pedrazzini et al., 2008; Jaboyedoff et al., 2009) and was constrained with displacement monitoring data (Froese et al., 2009a). The model proposed a toppling toward the east in the upper part of South Peak. A wedge shaped block located behind this toppling slope face is moving in a north-easterly direction. The back of

the unstable zone is bounded by a graben-like volume of subsiding material, which provides driving force acting on the wedge in front of it i.e. similar to a driving active wedge in a bi-planar mechanism (e.g., Coulthard, 1979). Frost wedging in the graben and wedge structures could also play an important role (Figure 3B). Large open cracks and intense fracturation in the lower part of the South Peak area could be related to the tectonic damage associated with the fold hinge and/or slope deformation associated with the instability in the upper part of South Peak (Figure 3A) (Pedrazzini et al., 2008).

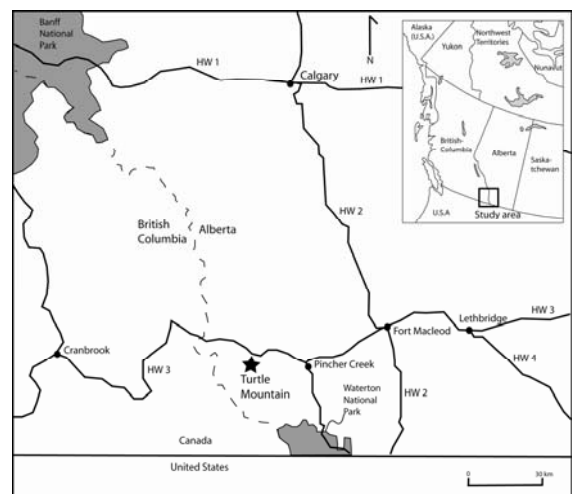


Figure 1. Location map of Turtle Mountain in Alberta

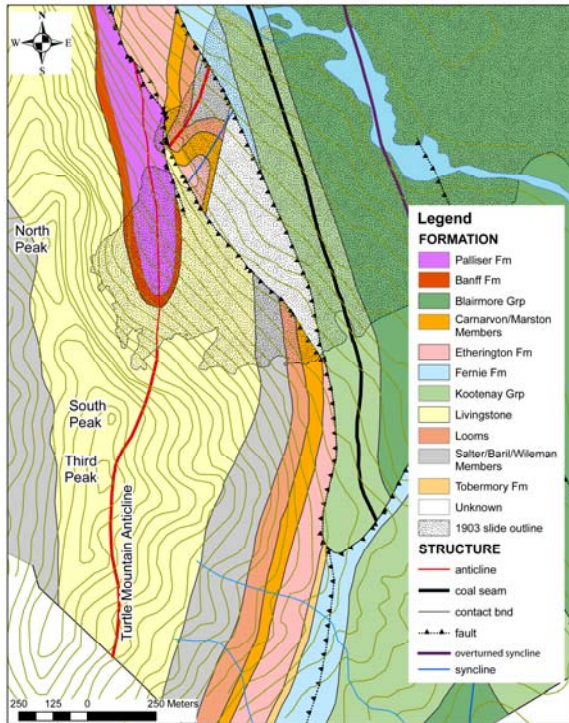


Figure 2. Geology of the Turtle Mountain area (based on Langenberg et al., 2007)

2 ROCK MASS CHARACTERISATION

The discontinuity measurements presented in this paper were collected using both scanline and subjective spot mapping at field stations in the upper South Peak area. The average orientation of the discontinuity sets is presented in Table 1. Discontinuity set J1 was only identified as a statistically important set in the lower section of South Peak via field measurements (Couture, 1998; Langenberg et al., 2007; Pedrazzini et al., 2008), borehole investigation (Spratt and Lamb, 2005), airborne LiDAR data (Jaboyedoff et al., 2009) and ground-based LiDAR and photogrammetry (Sturzenegger and Stead, 2009). Most of the subsequent analyses were performed both with and without J1 to assess its influence on slope stability. Discontinuity set J3 was observed to have a wide variability in orientation which was taken into account by considering two subsets J3' and J3/4. A typical outcrop containing discontinuity sets S0, J2, J3', and J4 is presented in Figure 4.

Table 1. Summary of discontinuity set orientations

Discontinuity set	Dip °	Dip Direction °	Comments
S0	52	280	
J1	45	020	Lower South Peak only. Orientation from Jaboyedoff et al., 2009
J2	56	060	
J3	41	127	
J3'	31	108	
J3/4	51	166	
J4	70	184	

The rock mass quality was characterised using the Geological Strength Index (GSI) introduced by Hoek and Brown (1997). The GSI estimates vary between 0 for a soil-like material and 100 for a massive rock. The GSI estimates are based on field observation at the outcrop scale of both the rock mass structures and the discontinuity surface conditions. Applications and limitations of the GSI have recently been discussed by Marinou et al. (2005) and Brideau et al. (2009).

Figure 5 summarizes the GSI estimates obtained in the South and Third Peak areas. The distribution is approximately normal with an average value between 45-55. According to Brideau et al. (2009) this value would correspond to a rock mass with structurally controlled stability. Figure 4 presents a typical rock outcrop in the South Peak area where at least four discontinuity sets are present. On the GSI chart this rock mass corresponds to a Very Blocky to Blocky/Disturbed/Seamy structure with Good discontinuity surface conditions.

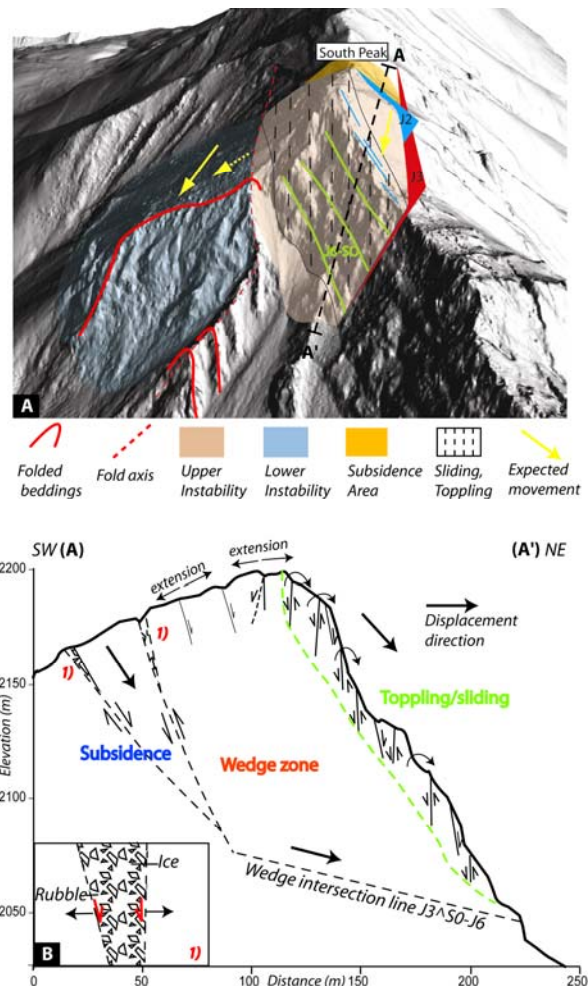


Figure 3. A) Hillshade of the South Peak DEM summarizing the conceptual model proposed based on surfaces identified in the airborne LiDAR, field observations and displacement monitoring data. B) Cross-section along A-A'.

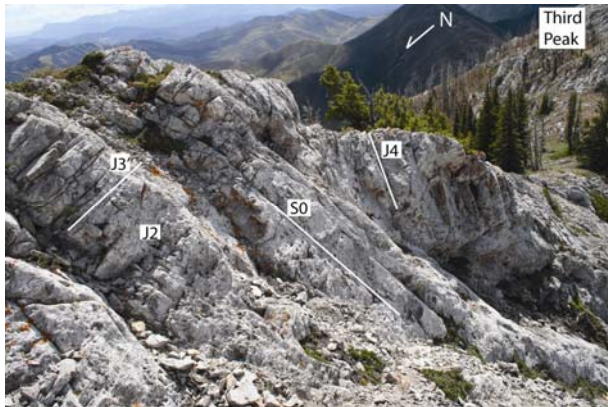


Figure 4: Major discontinuity sets observed in the South Peak area. The outcrop corresponds to a GSI estimate of 45-55.

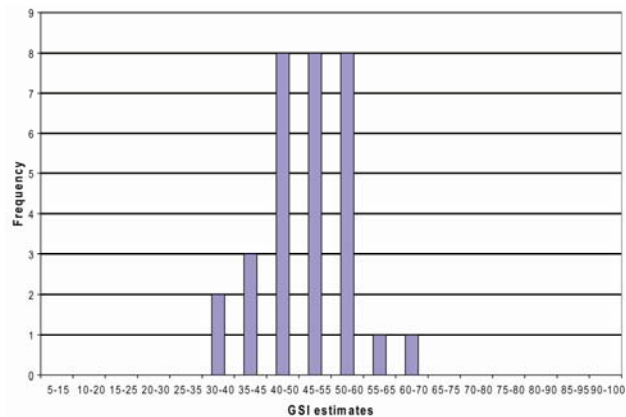


Figure 5. Histogram of the GSI estimates obtained in the South and Third Peak areas.

3 STABILITY ANALYSES

3.1 Kinematic analysis

A kinematic analysis is a rock slope stability test for simple structurally controlled failure modes such as planar sliding, wedge and toppling. It takes into consideration the orientation of the discontinuities, the slope orientation and the friction angle along the discontinuity surfaces. The stereographic techniques for the kinematic analysis of these simple failure modes are described in Wyllie and Mah (2004).

The kinematic analysis was conducted for the east (E) and east-southeast (ESE) faces of the South Peak promontory. The dip angle of the slope faces was assumed to be 60° to represent the steep upper portion of South Peak. The friction angle along all the discontinuity surfaces was assumed to be close to the residual value and it was estimated to be 30° as in the work of Benko and Stead (1998). Figure 6A demonstrates that sliding is feasible on the J3 and J3' discontinuity sets. Figure 6B highlights that wedge intersection between J2/J4, J2/J3', J4/J3' are feasible and J1/J3' marginally feasible. The toppling failure mechanism is feasible on discontinuities not associated with a major set and marginally feasible on some of the steeper discontinuities associated with S0 (bedding). No field evidence of widespread toppling along the bedding surfaces was observed.

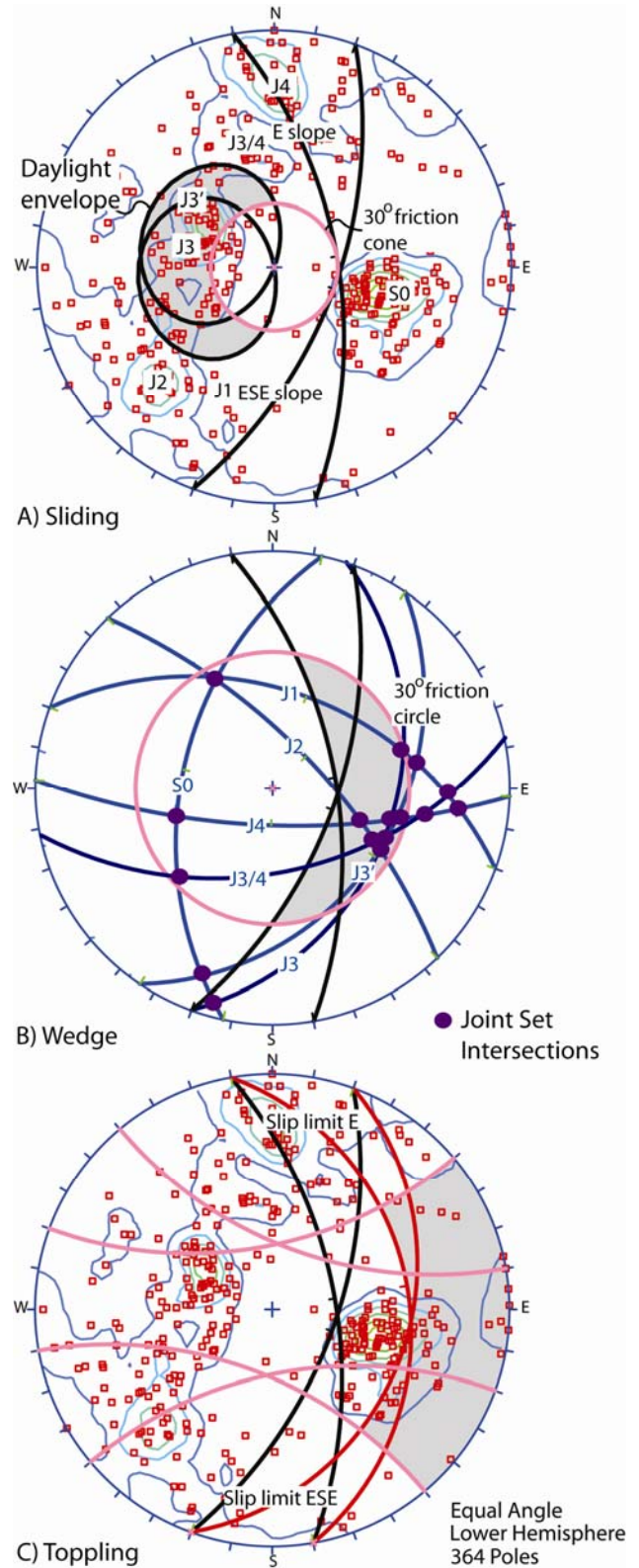


Figure 6: Kinematic analysis performed for the upper South Peak (slope E $60/080$, and slope ESE $60/110$ dip/dd).

3.2 Surface wedge limit equilibrium analysis

The limit equilibrium code Swedge, Rocscience (2006) was used to investigate the stability of rock wedges in the various rock slope faces forming South Peak. The combination analysis in Swedge uses a user defined list of discontinuities to calculate the factor of safety for each valid wedge intersection for a given slope face. The results of the combination analysis based on the discontinuities measured during fieldwork in the South Peak area are summarized in Table 2.

The slope assessed included the ESE and E portion of the South Peak promontory with dips of 40° (overall slope) and 60° (steep upper section). A NE slope section was also investigated to assess the stability along the sidescarp of the 1903 Frank Slide slope failure. The ESE face with a dip of 60° resulted in the highest number of unstable wedges. Figure 7 compares the wedge weight as a function of the factor of safety for the different slope surfaces. The results demonstrate that larger wedges can potentially be formed in the NE slope and that while the potential wedges in the ESE slope face are more numerous they tend to be smaller.

Table 2. Results of the surface wedge combination limit equilibrium analyses performed for the South Peak area using Swedge (Rocscience, 2006)

Slope assumed for surface wedge analysis	Valid wedges (% of valid combinations)	Stable wedges (% of valid wedges)	Unstable wedges (% of valid wedges)
ESE dip 40° 200 m high	13905 (21%)	11646 (84%)	2259 (16%)
ESE dip 60° 50 m high	22466 (34%)	14337 (64%)	8129 (36%)
E dip 40° 200 m high	13420 (20%)	12386 (92%)	1034 (8%)
E dip 60° 50 m high	23765 (36%)	16142 (68%)	7623 (32%)
NE dip 65° 200 m high	23143 (35%)	17429 (75%)	5714 (25%)

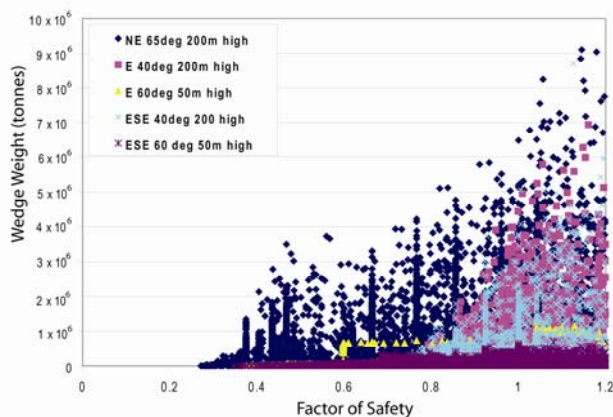


Figure 7. Scatter plot of the calculated maximum wedge weight as a function of the factor of safety (less than 1.2) for each valid combination in the different slope sections.

The software Matterocking (Jaboyedoff et al., 2004) compares the wedge intersection vector orientations with the topographic surfaces from a digital elevation model (DEM). Matterocking creates a surface layer file containing the average number of wedge intersections per unit cell in the DEM. These results can be displayed in a GIS environment. The input parameters are the azimuths, the dips and the spacing of the two discontinuity sets. Matterocking allows the influence of complex topography on the potential development of wedges to be assessed.

A Matterocking analysis was performed for all the discontinuity combinations identified as feasible for wedge failure in Figure 6B and for a wedge based on the intersection of S0 and J1 as observed by Predrazzini et al. (2008) in the lower South Peak area. Figure 8A demonstrates that the potential wedges created by the intersection of S0 and J1 tend to have a higher relative intensity per DEM cell on the NE portion of South Peak (1903 sidescarp) as proposed by the conceptual model. Figure 8B suggests that the intersection J3/J4 leads to a more widespread relative intensity per DEM cell with a weak concentration on the E and ESE portions of South Peak. These later results correspond to those obtain in the Swedge combination analysis.

3.3 Block theory

Block theory is a geometric and limit equilibrium analysis which considers the finiteness and removability of blocks based on the orientation of the discontinuity sets present and the excavation (slope) surfaces. Block theory was developed and applied to stereographic projection methods by Goodman and Shi (1985). There are five block categories in block theory: infinite, tapered, unconditionally or kinematically stable (resultant force vector oriented into the slope), stable with friction, and unstable with friction. The computer code used in this research Kbslope (Panttechnica, 2002) considers only sliding (planar and wedge) failure mechanisms and not rotational modes.

The results of the block theory analyses are summarised in Table 3. In the first analysis South Peak is represented using only two planes (E and ESE faces). This first analysis resulted in 17 finite blocks, 13 of which were stable without the removal of other blocks (11 tapered and 3 kinematically stable), 2 were stable with a friction angle of 30° along the discontinuities and 2 unstable blocks with friction. In the second analysis the same slope geometry was used but J1 was introduced resulting in a dramatic increase in the number of finite blocks (43), a modest increase in stable blocks with a 30° friction angle along the discontinuities (5), no increase in the number of unstable blocks with friction (2) was obtained. The third analysis added an additional slope surface (NE face or the 1903 sidescarp) to represent the topography of South Peak. The expanded excavation pyramid failed to significantly increase the number of finite blocks but doubled the number of unstable blocks with a 30° friction angle along the discontinuity surfaces (Figure 9). Similar block shape variations as shown in Figure 9A and B were present in all the block theory analyses conducted.

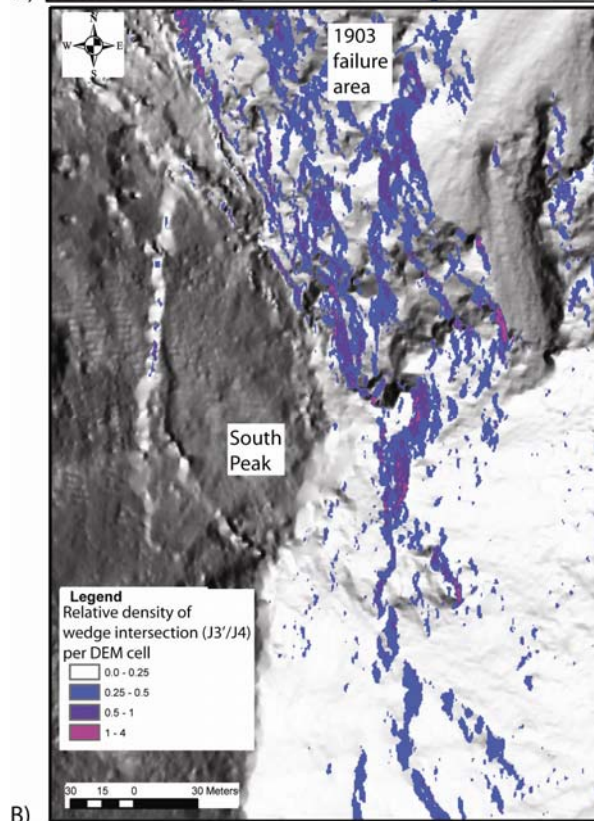
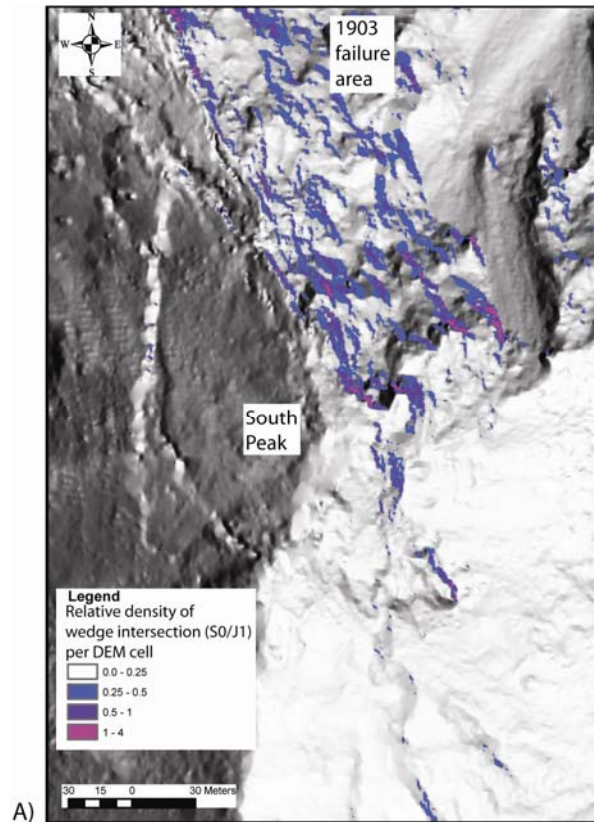


Figure 8: Relative density of wedge intersections per DEM cell in the area around South Peak for A) S0/J1 and B) J3'/J4.

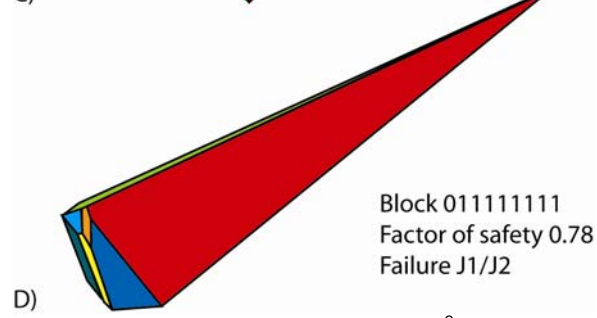
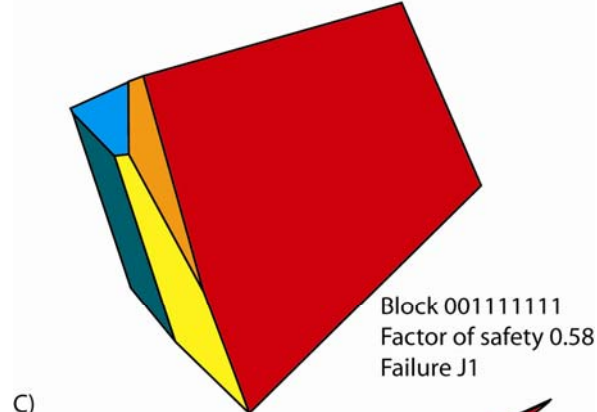
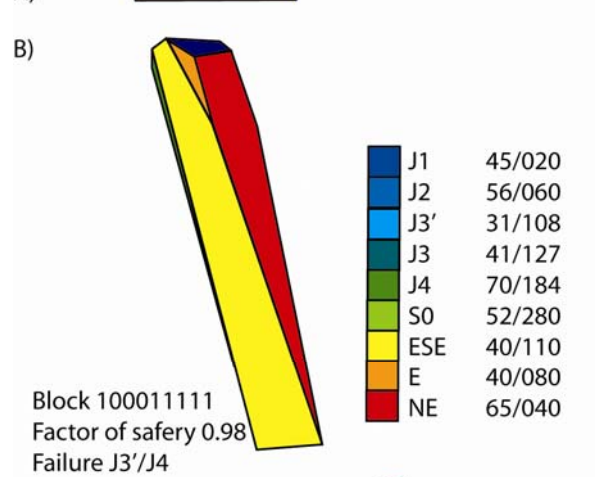
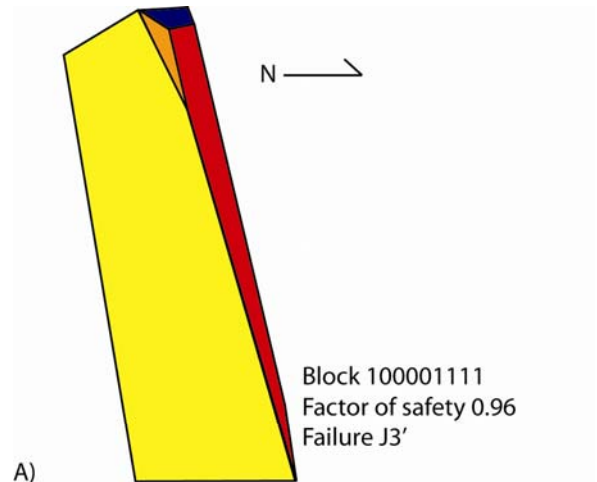


Figure 9: Unstable block with 30° friction along discontinuities.

Table 3: Summary of number of blocks from each category obtained for different combinations of slope geometries and discontinuity sets

	Finite	Tape- red	Kinema- tically stable	Stable with friction	Unstable with friction
E, ESE, J2, J3, J3', J4, S0	17	10	3	2	2
E, ESE, J1, J2, J3, J3', J4, S0	43	32	4	5	2
E, ESE, NE, J1, J2, J3, J3', J4, S0	47	34	5	6	4

3.4 Distinct element modelling

The three-dimensional distinct element code 3DEC (Itasca, 2008) was used to investigate the interaction of the discontinuity sets with a simplified topography of the South Peak area. In 3DEC, the material is represented as a collection of three-dimensional blocks under static or dynamic loading. The material strength of the blocks and bounding discontinuities are specified by the user. Large displacement and rotation along the discontinuities bounding the blocks are permitted.

The simplified topography of South Peak used in the 3DEC models is presented in Figure 10. It includes the average slope gradient of the lower parts, the steeper upper section and the narrow ridge of South Peak. The upper western face of the mountain was also included to evaluate its potential influence on the development of the large tension cracks observed in the field. The assumed input for the material and discontinuities properties used in the models are listed in Table 4. For these preliminary models the spacing for all discontinuity sets was kept constant at 75 metres.

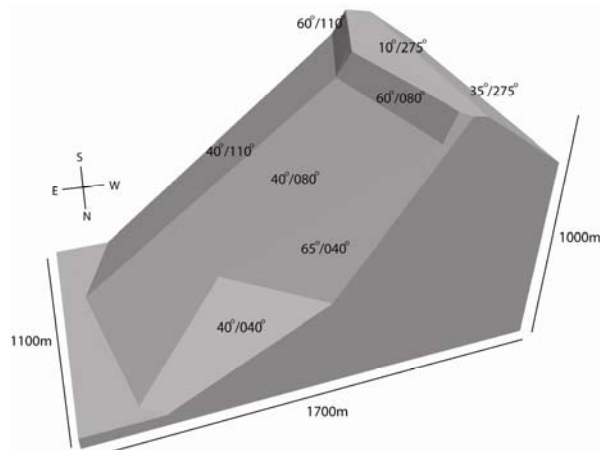


Figure 10. Simplified topography of the South Peak area used in the 3DEC models. Face orientations are listed as dip / dip direction.

The first model (Figure 11) included the four main discontinuity sets and two subsets identified in the upper South Peak area (S0, J2, J3, J3', J3/4, J4). The

displacement contour plots (Figure 11A and B) show that minor wedge instabilities are simulated along the steeper upper South Peak within a broad semi-circular zone with deformation between 0.2 and 0.4m (results after 20 000 calculation steps).

Table 4: Material and joint properties used in the 3DEC models

Material properties	
Density (kg/m ³)	2700
Bulk modulus (GPa)	1.5
Shear modulus (GPa)	1
Joint properties	
Shear stiffness (GPa/m)	1
Normal stiffness (GPa/m)	1
Friction angle (°)	30
Cohesion (MPa)	0
Tensile strength (MPa)	0

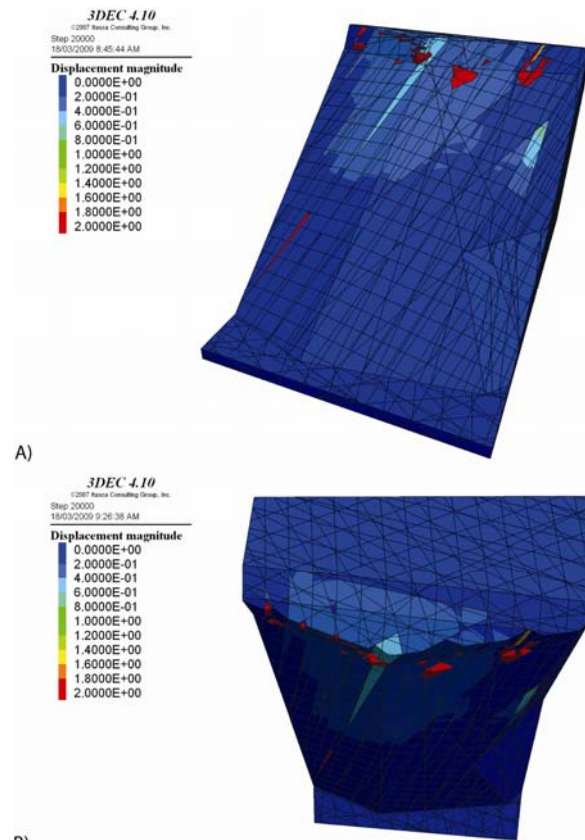


Figure 11. Calculated displacement contours in 3DEC after 20 000 calculation steps. Model with S0, J2, J3, J3', J3/4, J4 discontinuity sets (30° friction angle). A) perspective view. B) top view

In the second model (Figure 12) the discontinuity set J1 was introduced to evaluate its influence on the slope stability conditions. The displacement contour plots (Figure 12A and 12B) show a large scale slope failure with some of the blocks even sliding outside the model boundaries after 20 000 calculation steps. Figure 12B

highlights the irregular (saw-tooth or stepped) appearance of the backscarp obtained in this second model.

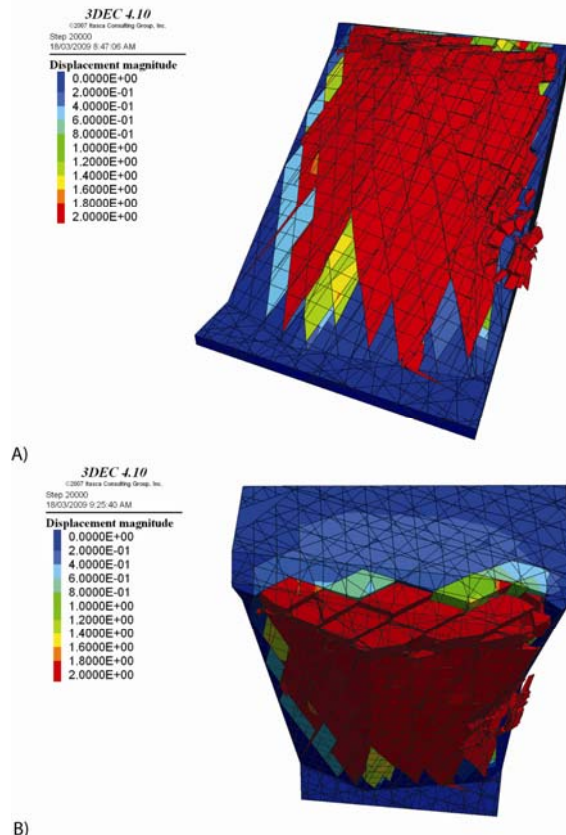


Figure 12. Calculated displacement contours in 3DEC after 20 000 calculation steps. Model with S0, J1, J2, J3, J3', J3/4, J4 discontinuity sets (30° friction angle). A) perspective view. B) top view.

4 DISCUSSION

4.1 Influence of 3-dimensional topography on slope stability analysis

The South Peak promontory shape is difficult to incorporate in simple slope stability analyses. For example, in the kinematic analysis two slope surfaces were considered simultaneously to account for the expanded daylight envelope and increase kinematic freedom. A similar approach has been used by Yoon et al. (2002) for sliding (planar and wedge) failure mechanisms. This approach has never been rigorously validated for a toppling mechanism.

The Swedge combination analysis performs a wedge kinematic analysis for each combination of two discontinuity surfaces and one constant slope orientation. The Swedge analysis therefore had to be performed for each of the slope surfaces of interest in turn without considering any potential interaction between the slope surfaces. The Matterocking analysis takes into account the complex topography by performing a kinematic wedge analysis for two average discontinuity orientations within each cell of the slope surface in the DEM. The drawback of the Matterocking analysis is that it only considers the

average orientation of the discontinuity sets and cannot account for the natural variability in orientation. The Swedge combination and Matterocking analyses can be considered to be complementary and both need to be considered in the case of complex topography such as at South Peak.

The block theory analysis performed with Kbslope also has some limitations when applied to complex topography. A fundamental assumption of block theory is that the blocks and topography are convex. In the case of South Peak this requirement was met. A second limitation of the method is that the location of the surface excavation can only be specified using a point in space. The extent or relation of the planes to each other cannot be defined. This leads to blocks made up of thin slivers of the eastern slope surface plane and dominated by east-southeast and northeast slope surface planes as in Figure 9A and B or discontinuous ground surfaces as in Figure 9D neither are realistic. The blocks presented in Figure 9 are still finite, removable and unstable with a friction angle of 30° but their actual shape might be slightly different due to more realistic topographic constraints (in Kbslope the block volume is maximized using the given plane orientations).

4.2 The role of J1 on the slope stability

As mentioned in section 2 the discontinuity set J1 was recorded in the upper section of South Peak but did not appear to be statistically significant. In the kinematic analysis considering the east and east-southeast face the presence of J1 did not influence the sliding or toppling mechanism but resulted in a marginally feasible wedge in combination with J3' (Figure 6B). In the Matterocking analysis the presence of J1 was shown to lead to development of potential wedges in the northeast face (1903 scar) of South Peak (Figure 8). The potential influence of J1 on slope stability was also emphasized by Jaboyedoff et al. (2009) to explain the failure mechanism of the 1903 slide. The consideration of J1 in the block theory analysis increased the number of finite blocks and stable blocks with a friction angle of 30° (Table 3). It is in the 3DEC analysis that the importance of J1 appeared to be the greatest. The 3DEC models showed minor slope instability on the steep upper part when J1 was absent (Figure 11) and large scale slope failure when it was present (Figure 12). While the displacement are much greater than observed and volume of the unstable mass is overestimated (Froese et al., 2009a) the model captures the various direction of movement observed in the displacement monitoring data (Froese et al., 2009b). More field data needs to be collected on the surface condition and persistence of the J1 discontinuity set in the upper South Peak area to allow further and more constrained representation in 3DEC.

4.3 Comparisons between the conceptual model and numerical modelling results

This paper has presented the preliminary results of field data and slope stability analysis to assess a conceptual slope stability model of South Peak. The wedge failure zone in the northeast face proposed in the conceptual slope stability model by Pedrazzini et al. (2008) and

Jaboyedoff et al. (2009) of South Peak was reproduced in limit equilibrium, block theory and 3-dimensional distinct element analyses. The toppling failure mechanism was feasible according to the kinematic analysis of the field data but was not explicitly recognised in the 3-dimensional distinct element models. This can be attributed to the block size scale effects in the model (1000 m's) and blocks (10's m) while the toppling was observed and predicted to be a local failure mode. Finally subsidence in the rear (western side) of South Peak was observed to develop in some of the 3-dimensional distinct element models. The mechanical analysis presented in this paper therefore support the general behaviour proposed by the conceptual model. The distinct element model also provides a new constraint to the conceptual model showing that the subsidence in the upper section of South Peak is potentially linked both to the movement in the lower section and to the presence of J1.

5 CONCLUSION

This paper summarises the field data collected by the authors in 2008 and preliminary numerical modeling based on it. The rock mass quality in the upper part of South Peak was determined to have an average GSI value of 45-55. The results presented have highlighted the role of the complex topography at South Peak and the importance of the J1 discontinuity set on the slope stability conditions. The preliminary 3-dimensional distinct element model presented supports both the general behaviour in the previously proposed conceptual model and the displacement monitoring data. Current displacements are modeled as wedge sliding, toppling and subsidence. Further modelling assuming a more realistic J1 distribution is planned after additional fieldwork has been conducted. The use of this preliminary analysis in indication required field data collection is emphasised.

ACKNOWLEDGEMENTS

The authors would like to acknowledge discussions with M. Sturzenegger on the discontinuity pattern at South Peak and the assistance in the field by D. vanZeyl and F. Humair. Funding was provided in part by the Alberta Geological Survey and the FRBC Resource Geoscience and Geotechnics Endowment Fund to D. Stead. R. Couture provided comments on the manuscript.

REFERENCES

Benko, B., Stead, D., 1998. The Frank Slide: A reexamination of the failure mechanism. *Canadian Geotechnical Journal*, 35: 299-311.

Brideau, M.-A., Yan, M. and Stead, D., 2009. The role of tectonic damage and brittle rock fracture in the development of large rock slope failures. *Geomorphology*, 103(1): 30-49.

Coulthard, M.A., 1979. Back-analysis of observed spoil failures using a two-wedge method. 83, CSIRO technical report 83. 20p.

Couture, R., 1998. Contributions aux aspects physiques et mécaniques des écroulements rocheux. Ph.D. Thesis, Université de Laval, Laval, Québec (QC).

Cruden, D.M. and Martin, C.D., 2007. Before the Frank Slide. *Canadian Geotechnical Journal*, 44: 765-780.

Cruden, D.M., and Krahn, J., 1973. A re-examination of the geology of the Frank Slide. *Canadian Geotechnical Journal* 10: 581-591.

Froese, C.R., Moreno, F., Jaboyedoff, M., and Cruden, D.M., 2009a. 25 years of movement monitoring on South Peak, Turtle Mountain: understanding the hazard. *Canadian Geotechnical Journal* 46: 256-269.

Froese, C.R., Jaboyedoff, M., Pedrazzini, A., Hungr, O., and Moreno, F., 2009b. Hazard mapping for the eastern face of Turtle Mountain, adjacent to the Frank Slide, Alberta, Canada. In: *Landslide Processes* Strasbourg, France p. 283-289.

Goodman, R.E., and Shi, G.H., 1985. Block theory and its application to rock engineering. Prentice-Hall. 338 p.

Hoek, E. and Brown, E.T., 1997. Practical estimates of rock mass strength. *International Journal of Rock Mechanics and Mining Sciences*, 34(8): 1165-1186.

Itasca, 2008. 3DEC v. 4.1, Itasca Consulting Group, Minneapolis, Minnesota

Jaboyedoff, M., Couture, R. and Locat, P. 2009. Structural analysis of Turtle Mountain (Alberta) using digital elevation model: toward a progressive failure. *Geomorphology*, 103(1): 5-16

Jaboyedoff, M., Baillifard, F., Philipposian, F., and Rouiller, J.-D., 2004. Assessing fracture occurrence using "weighted fracturing density": a step towards estimating rock instability hazard. *Natural Hazards and Earth System Sciences* 4: 83-93.

Langenberg, C.W., Pana, D., Richards, B.C., Spratt, D.A., and Lamb, M.A. 2007. Structural geology of the Turtle Mountain area near Frank, Alberta. EUB/AGS Science Report 2007-01, 30 p.

Marinos, V., Marinos, P., and Hoek, E., 2005. The geological strength index: Applications and limitations. *Bulletin of Engineering Geology and the Environment*, 64: 55-65.

Moreno, F., and Froese, C.R., 2006. Turtle Mountain Field Laboratory, Monitoring and Research Summary Report. EUG/AGS Earth Science Report 2006-07n

Pantechnica, 2002. Kbslope, Pantechnica Corporation, Chaska Minnesota

Pedrazzini, A., Jaboyedoff, Froese, C., Langenberg, W., and Moreno, F., 2008. Structures and failure mechanisms analysis of Turtle Mountain, *Canadian Conference on Geohazards IV*, Quebec City, Quebec. p. 349-356.

Rocscience, 2006. Swedge v5.0, Rocscience Inc. Toronto, Ontario

Spratt, D. and Lamb, M., 2005. Borehole data interpretation and orientations: Turtle Mountain Monitoring Project. WP15b, University of Calgary, 15p.

Sturzenegger, M., and Stead, D., 2009. Quantifying discontinuity orientation and persistence on high mountain rock slopes and large landslides using terrestrial remote sensing techniques. *Natural Hazards and Earth System Sciences* 9: 267-287.

Wyllie, D.C., and Mah, C.W., 2004. Rock Slope Engineering, 4th Edition. SponPress, New York, 431 p.

Yoon, W.S., Jeong, U.J. and Kim, J.H., 2002. Kinematic analysis for sliding failure of multi-faced rock slopes. *Engineering Geology*, 67: 51-61.